

## *Supplementary Material*

# **Quantifying parameter uncertainty in a large-scale glacier evolution model with a Bayesian model – Application to High Mountain Asia**

**David R. Rounce\***, Tushar Khurana, Margaret B. Short, Regine Hock, David E. Shean, and Douglas J. Brinkerhoff

\* **Correspondence:** David Rounce: [drounce@alaska.edu](mailto:drounce@alaska.edu)

### **TABLE OF CONTENT**

#### **1. Supplementary Figures**

- **Figure S1:** Regional prior distributions for the temperature bias. (*Page 2*)
- **Figure S2:** Regional prior distributions for the precipitation factor. (*Page 3*)
- **Figure S3:** Observed, posterior predictive, prior, and posterior distributions, and mass balance versus model parameters for glacier RGI60-13.45048. (*Page 4*)
- **Figure S4:** Observed, posterior predictive, prior, and posterior distributions, and mass balance versus model parameters for glacier RGI60-15.10755. (*Page 5*)
- **Figure S5:** Observed, posterior predictive, prior, and posterior distributions, and mass balance versus model parameters for glacier RGI60-15.12457. (*Page 6*)
- **Figure S6:** Convergence diagnostics (Monte Carlo error and effective sample size) for all glaciers in High Mountain Asia. (*Page 7*)
- **Figure S7:** Comparison of observed and mean mass balance using the calibration scheme of Huss and Hock (2015). (*Page 8*)

## 1 Supplementary Figures

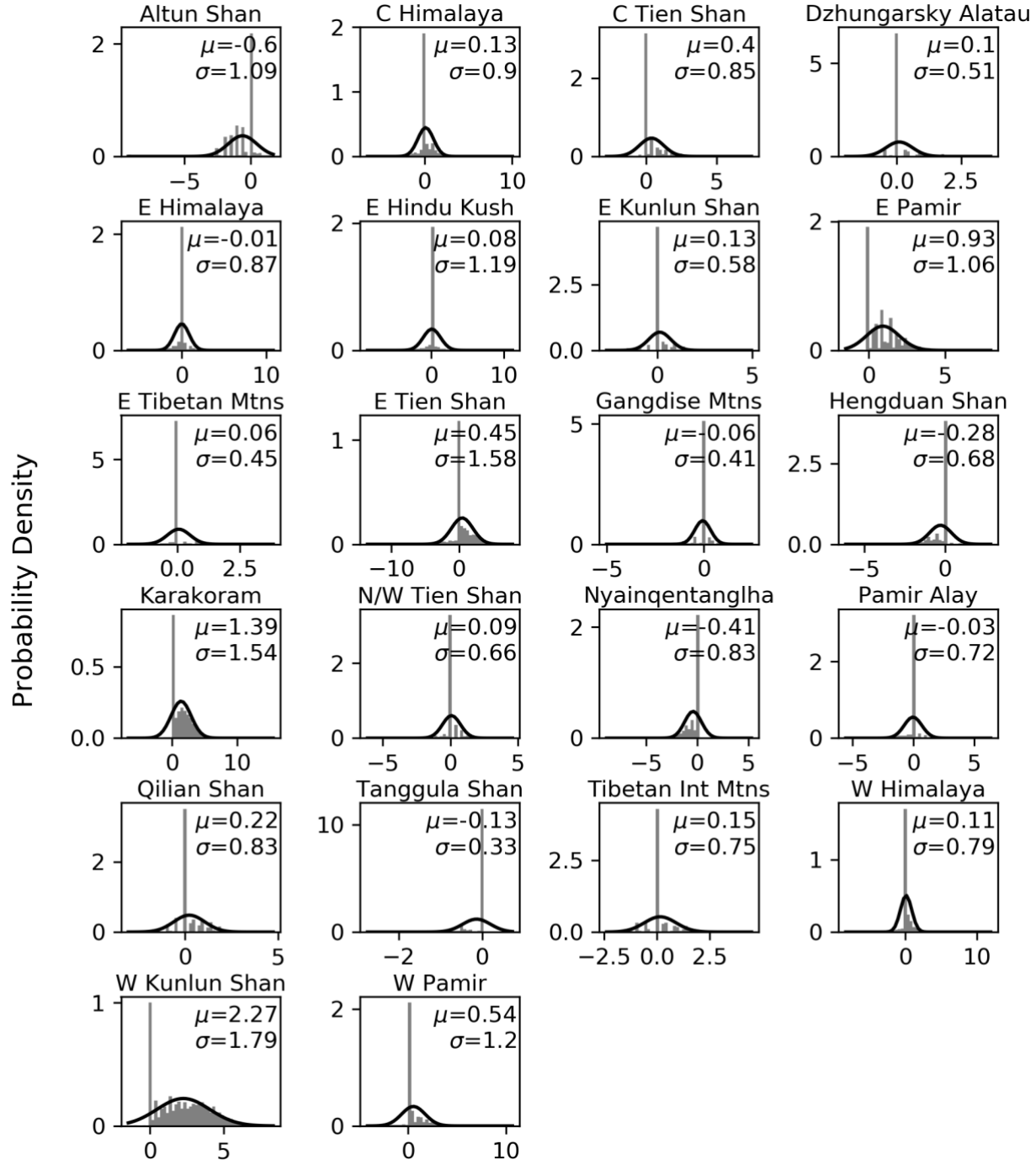


**Figure S1.** Marginal prior distribution for the temperature bias for each region (black) assuming a gamma distribution based on the mean and standard deviation from the results of the simplified optimization scheme (grey).

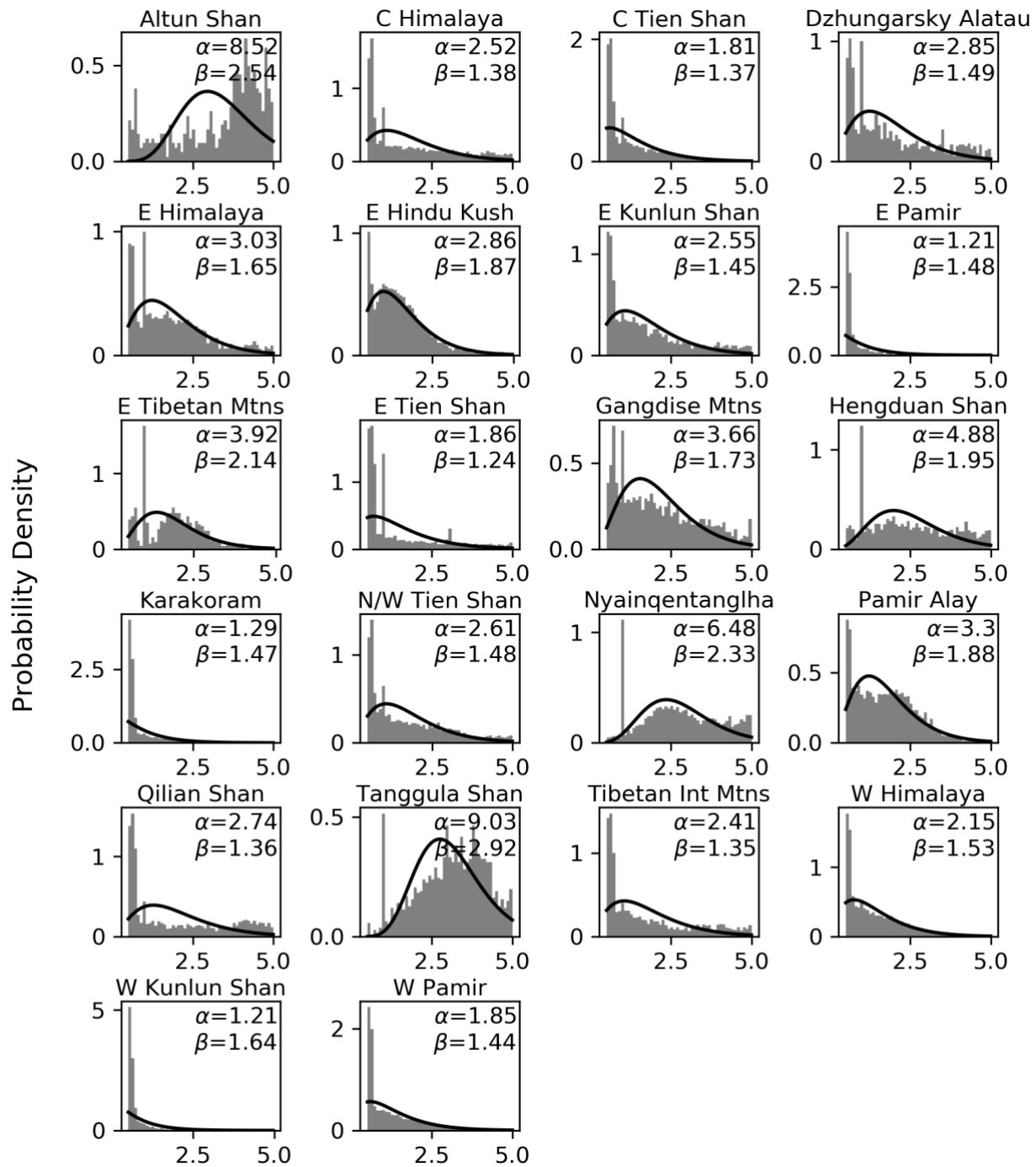


**Figure S2.** Marginal prior distribution for the precipitation factor for each region (black) assuming a gamma distribution based on the mean and standard deviation from the results of the simplified optimization scheme (grey).

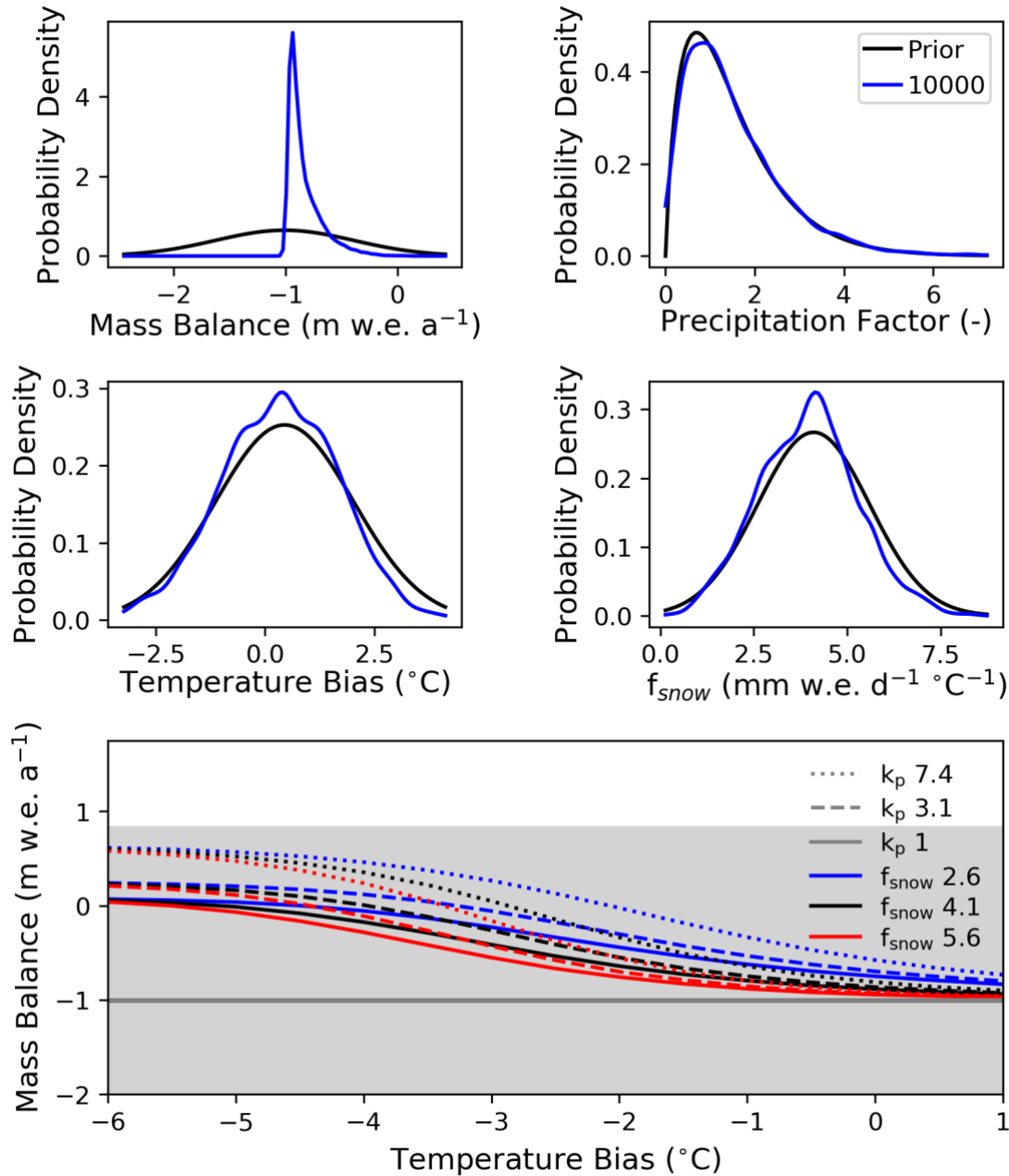


**Figure S3.** Observed and predictive posterior distribution for the mass balance along with prior and posterior distributions for the precipitation factor, temperature bias, and degree day factor of snow ( $f_{snow}$ ) for glacier RGI60-13.45048 for a single chain of 10,000 steps, and subplot showing the mass balance versus model parameters.

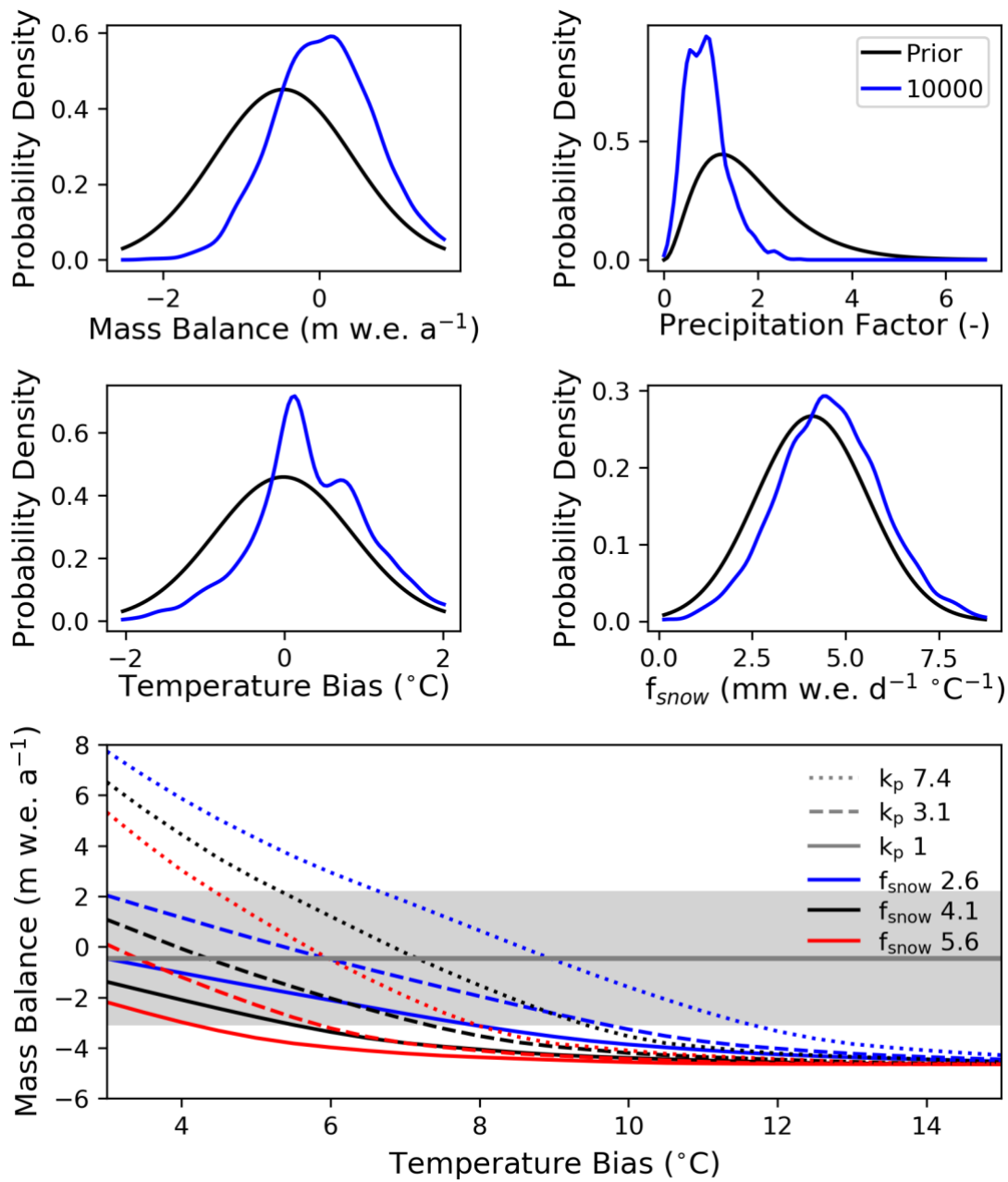


**Figure S4.** Observed and predictive posterior distribution for the mass balance along with prior and posterior distributions for the precipitation factor, temperature bias, and degree day factor of snow ( $f_{snow}$ ) for glacier RGI60-15.10755 for a single chain of 10,000 steps, and subplot showing the mass balance versus model parameters.

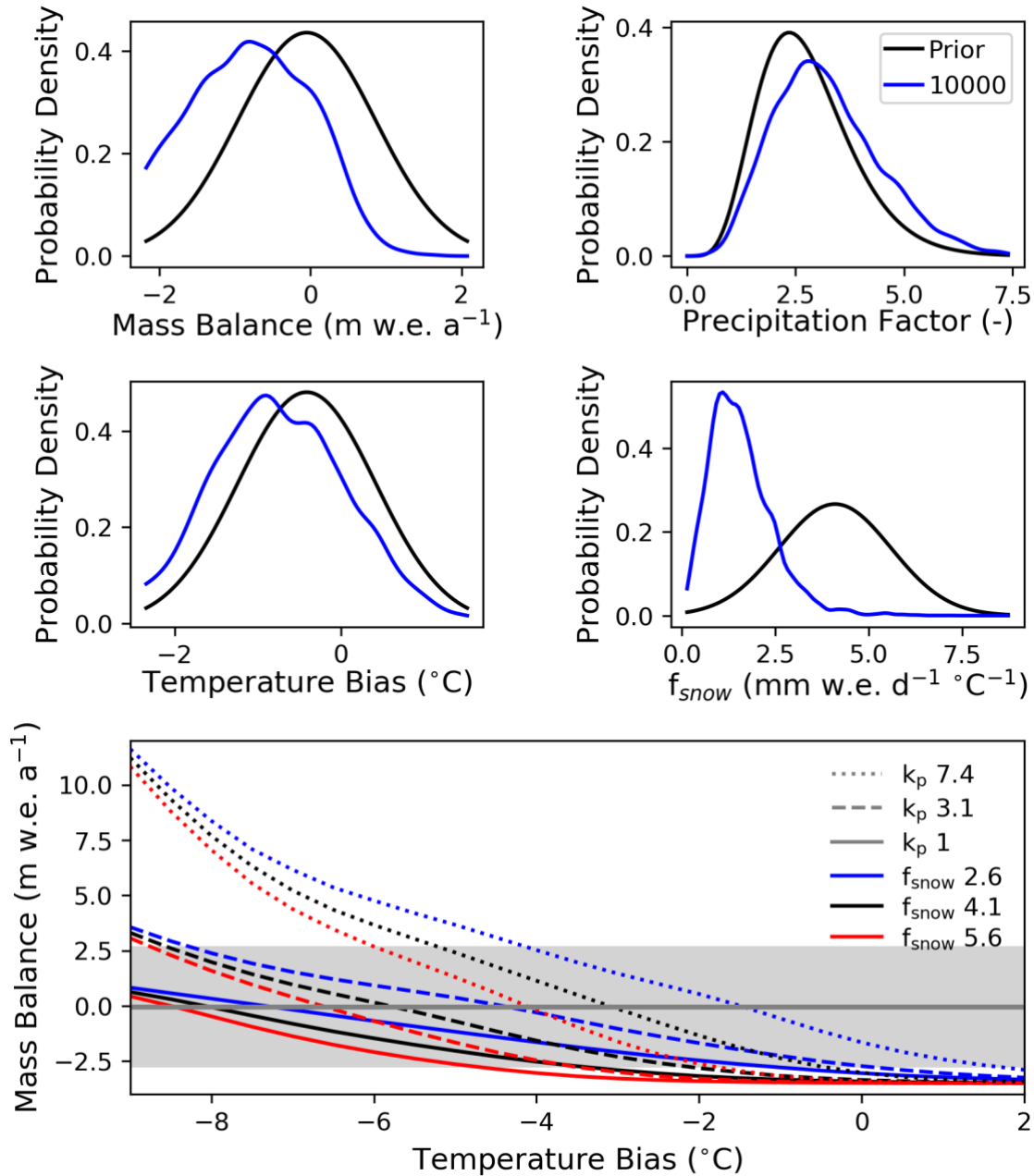


**Figure S5.** Observed and predictive posterior distribution for the mass balance along with prior and posterior distributions for the precipitation factor, temperature bias, and degree day factor of snow ( $f_{snow}$ ) for glacier RGI60-15.12457 for a single chain of 10,000 steps, and subplot showing the mass balance versus model parameters.

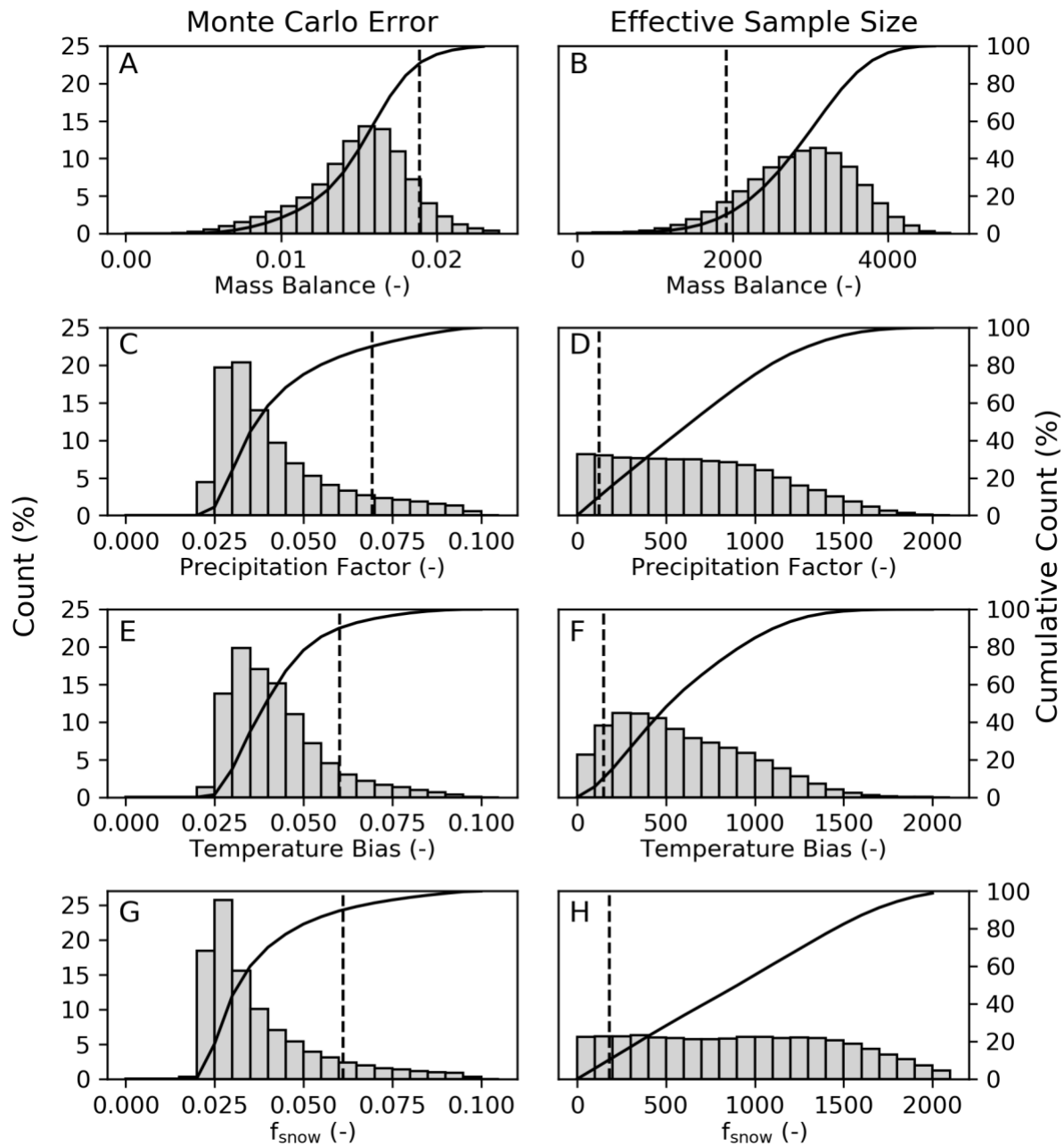


**Figure S6.** Histogram and cumulative percentage of Monte Carlo error and effective sample size for the mass balance (A,B), precipitation factor (C,D), temperature bias (E,F), and degree-day factor of snow ( $f_{snow}$ ) (G,H) for all the glaciers in High Mountain Asia. Solid black lines show the cumulative percentages, and dashed black lines show the 90-percentile value for Monte Carlo error and 10-percentile value for effective sample size. The Monte Carlo error is normalized by the standard deviation of the posterior distribution.

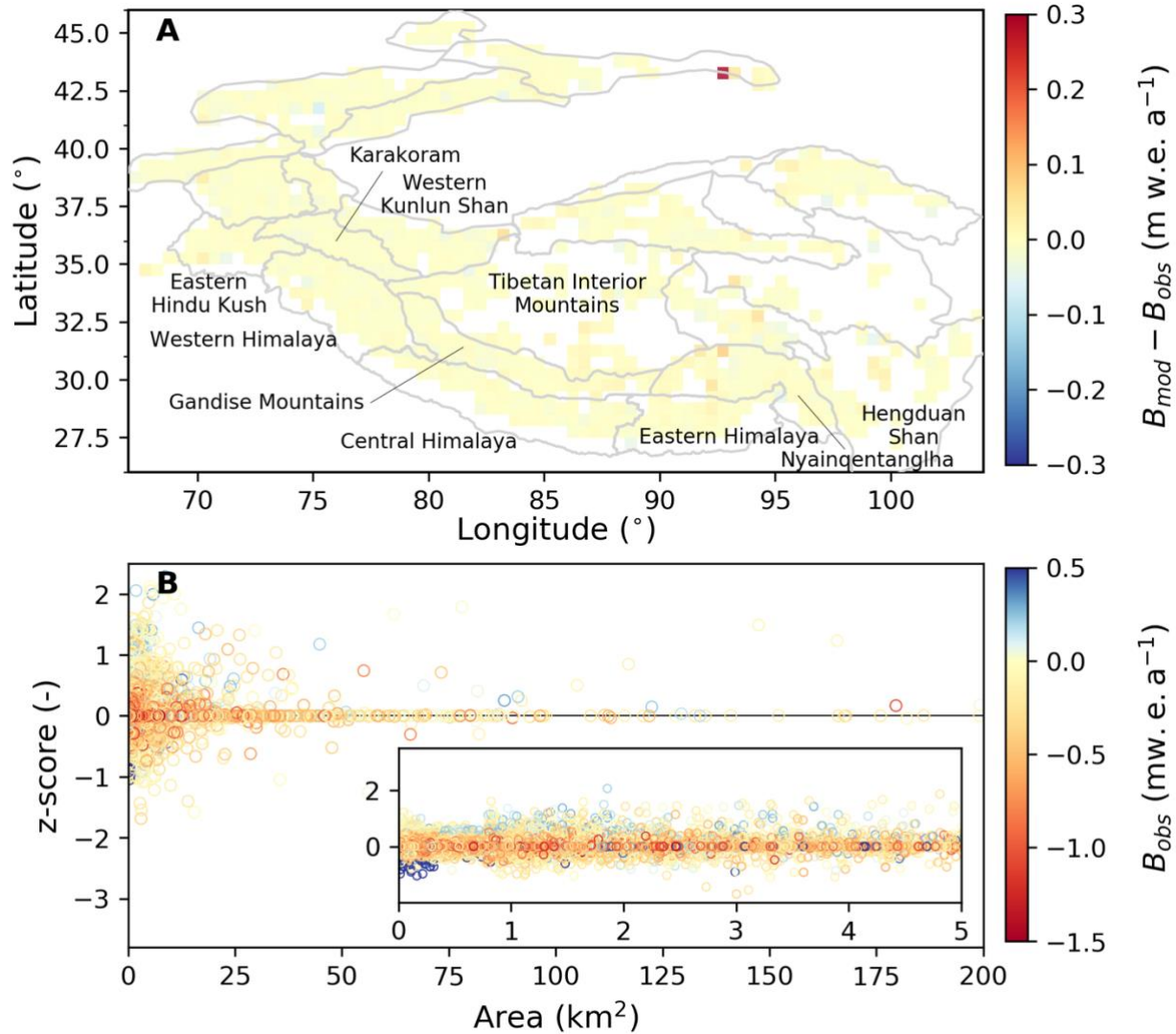


**Figure S7.** The difference between the observed ( $B_{obs}$ ) and mean ( $B_{mod}$ ) mass balance (A) showing the spatial distribution aggregated to  $0.5^\circ$  grids and (B) as a function of glacier area for every glacier in High Mountain Asia using the calibration scheme of Huss and Hock (2015). Grey outlines show 22 subregions from Bolch and others (2019).